


AN ABSTRACT OF THE THESIS OF

Peter E. Perkins for the M.S.
(Name of Student) (Degree)

in Electrical Engineering presented on June 9, 1967
(Major) (Date)

Title: The Design and Development of a Noncompressing Post-
deflection Acceleration Method for Cathode-ray Tubes

Abstract approved:


(Signature)
Donald L. Amort

A short history is given of cathode-ray tubes, from the earliest laboratory tubes available during the early 1900's through present day high performance tubes. Special attention is paid to the development of post-deflection acceleration types especially band-type PDA tubes and an improvement on that type known as the helix-type PDA tube.

One of the most severe complications of the band or helix-type PDA tube has been scan compression. Analysis of this problem has led directly into the noncompressing method developed here. A model of this noncompressing method, i.e. the voltage and gradient between two spheres, is applied to a practical system. Some of the constraints of the practical system including the problem of two

virtual sources for the beam, the design of the field-forming element and the limitations on the application of the required boundary conditions, have complicated the design somewhat. These constraints have not prevented the achievement of a close approximation to the voltage and gradient required from the analysis.

Evaluation of this new noncompressing CRT (now called a mesh-type tube) shows it to be superior to the older types of PDA tubes in every respect except for minimum spot size. In addition to the mesh tube's low sensibility and high writing speed, the mesh tube is compact and adapts nicely to the small package size required for modern day equipment.

The Design and Development of a
Noncompressing Post-deflection Acceleration Method
for Cathode-ray Tubes

by

Peter Eugene Perkins

A THESIS

submitted to

Oregon State University

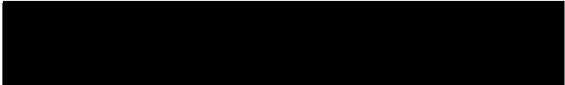
in partial fulfillment of
the requirements for the

degree of

Master of Science

June 1968

APPROVED:


Assistant Professor of Electrical and Electronics Engineering
in charge of major


Head of Department of Electrical and Electronics Engineering


Dean of Graduate School

Date thesis is presented June 9, 1967

Typed by Virginia Jones for Peter Eugene Perkins

ACKNOWLEDGMENT

I would like to express my appreciation to the many people who have contributed to this work in many different ways. First, to the CRT Engineering staff at Tektronix, Inc., who served both as counsellor and devil's advocate during the course of the analysis and design; secondly, to many CRT people there, each of whom has contributed in ways too numerous to mention. I would express my thanks for their assistance. I would like to especially mention Egon Elssner and Orv Olson who, on separate occasions, directed this work effort.

To my wife, Ruth, and my family I am deeply grateful for their patience and forbearance during this extended period of schooling.

Finally, I am thankful for the encouragement of my father, Eugene T. Perkins, toward high scholastic goals and excellence through many years of schooling.

TABLE OF CONTENTS

I.	Introduction.	1
	Early History.	1
	A Short CRT History.	2
	Development of Band-type PDA Schemes	5
	Development of Helix-type PDA Schemes.	12
	The Problem Defined.	16
II.	Theory of Operation of This Noncompressing Method	19
	A Simple Model	19
	The Model Refined.	25
III.	Practical Consideration	28
	Application to a Closed System	28
	System Restrictions.	31
IV.	Evaluation of the Final System.	37
	Performance Comparisons.	37
	Summary.	42
V.	Bibliography.	44
VI.	Appendix.	47

LIST OF FIGURES

1.	Luminance vs. accelerating voltage for P31 phosphor. . . .	3
2.	Comparison of single and multiband deflection performance with PDA voltage	7
3.	Comparison of single and multiband deflection performance with PDA voltage	7
4.	Comparison of scan compression performance for various PDA tube types	9
5.	Comparison of scan compression performance for various PDA tube types	9
6.	Comparison of deflection vs. deflection angle tangent for band and helix type PDA tube	11
7.	Compression ratio vs. PDA ratio for helix PDA tube	11
8.	Comparison of linearity characteristics for monoaccelerator and helix PDA CRT's.	13
9.	Scan compression in single band PDA tube	15
10.	Scan compression in helix PDA tube	15
11.	Definition of coordinate directions for spherical coordinate system.	20
12.	Equipotentials around a sphere	22
13.	Potential and potential gradient around a sphere	22
14.	Potential and potential gradient for an accelerating field between two spheres.	24
15.	Voltage and gradient between two spheres	27
16.	Electrolytic tank plots showing distribution of equipotential in the bulb.	29
17.	Comparison of measured voltage and gradient to calculated values	30
18.	Depiction of center of deflection for a pair of deflection for a pair of deflection plates.	33

LIST OF FIGURES, Continued--

19.	Spot size vs. mesh pitch	33
20.	Comparison of scan compression factors for standard helix and mesh type PDA tube	36
21.	Trace width comparison for helix and mesh PDA tube	36
22.	Deterioration of resolution vs. PDA ratio for the mesh PDA tube	38
23.	Change of trace width with PDA ratio for the mesh PDA tube	38
24.	Comparison of linearity characteristics for monoaccelerator and helix PDA CRT's.	41
A1.	Relating beam parameters to writing speed calculations	48
A2.	Calculated writing speed performance	53

THE DESIGN AND DEVELOPMENT OF A
NONCOMPRESSING POST-DEFLECTION ACCELERATION METHOD
FOR CATHODE-RAY TUBES

I. INTRODUCTION

Any short history of cathode-ray tubes (CRT's) should probably point the reader to the recentness of any simple understanding of the nature and use of electrons.

Early History

In 1859, Plucker used a magnetic field to move a greenish glow around on the walls of a sealed tube. In 1868, his student, Hittorf, saw that the fluorescence could be masked by any opaque object and deduced it to be a form of radiation proceeding in straight lines from the cathode (he called them cathode rays). Crooks' work was similar to Hittorf, his contemporary. In 1879, Crooks published his work on the famous Maltese Cross tube. He was the first to show the mutual repulsion of two "cathode rays" and showed that they were negatively charged.

In 1892, Hertz, Hess, and Lenard showed that the particles (or waves, since there was some controversy) could penetrate thin films and even leave the tubes. About that same time, Perrin tried to show that they were particles by collecting them in an electroscope.

In 1897, J. J. Thompson proved that the particles were bound up with the charge and demonstrated an electrostatic deflection system. He was the first to measure the charge-to-mass ratio, e/m . It was in

1909 that Millikan first performed his e/m measurement with the famous oil drop experiment.

A Short CRT History: The use of cathode rays for display purposes.

The first laboratory tubes were produced by Braun, in 1897, using a cold cathode, a wire anode, a restricting aperture, and Willemite coated mica screen. These tubes used magnetic deflection. Commercial tubes were first made available by 1903 by Cossor in England; they were improved in that they used electrostatic deflection plus an internal conductive coating to keep the walls of the envelope from charging. For the next several decades, these simple types of tubes, with some small improvements, were the mainstay for the art. The tubes were as much a laboratory curiosity as a measuring or display tool.

It was in 1922 that Western Electric introduced their type 224 CRT. This was a gas-focused tube that used an oxide-coated platinum ribbon cathode. The cathode was coiled so that the oxide coating was not beneath the grid opening and, therefore, not subject to ion bombardment during operation of the tube. This tube, which was known as the "Johnson tube", had a useful operating life of about 100 hours. This popular type introduced many early experimenters to the concept of visually displaying electrical phenomena.

Gas focusing, originally suggested by VanderBijl, was used until 1926 when Busch demonstrated both magnetic and electrostatic focusing of electron beams.

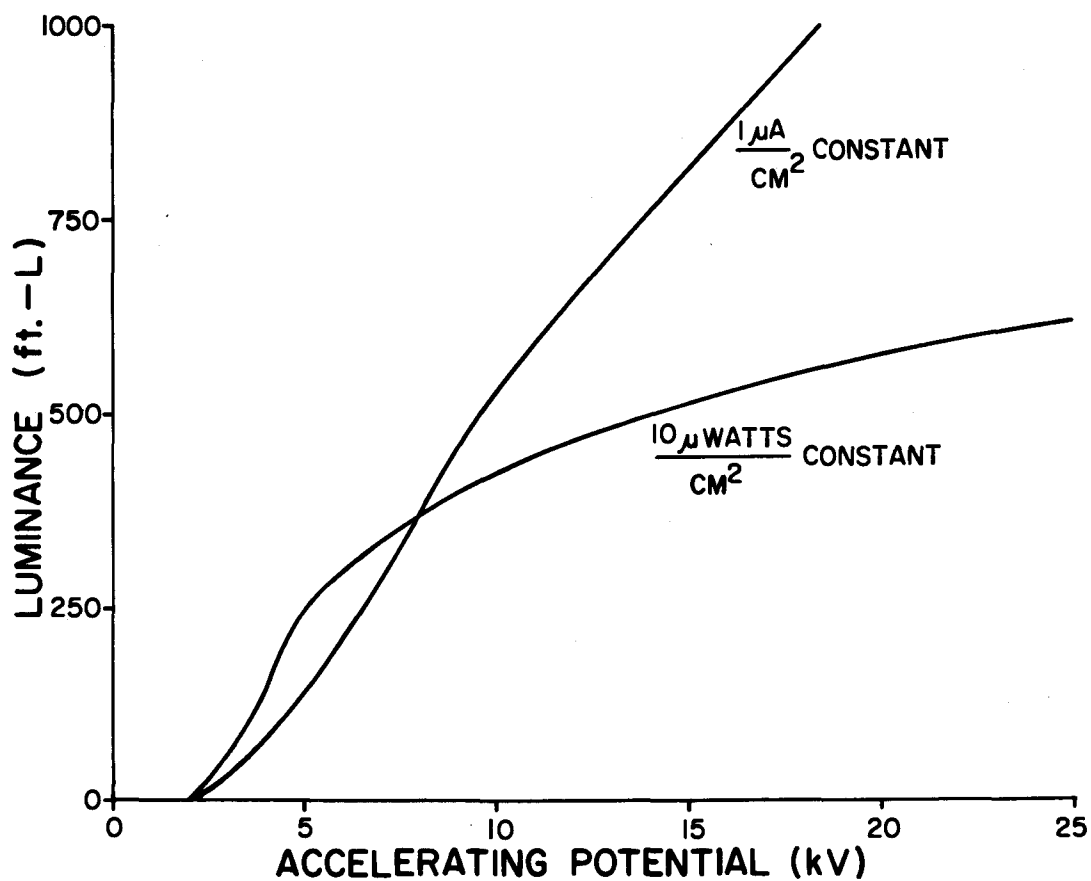


FIG. 1
LUMINANCE vs. ACCELERATING VOLTAGE
FOR P31 PHOSPHOR.

A variety of tubes of the modern form; i.e., with apertured focusing systems along with shielded (noninteracting) deflection systems, etc., were available about 1932. These CRT's were principally monoaccelerators and were normally operated in the 1-2 kV region. The tubes worked comfortably for repetitive displays of low to medium frequencies. They suffered badly from a luminance standpoint when applied to single-shot or high frequency displays (in the 200 to 500 kHz region).

The relationship of luminance to accelerating potential shown in Figure 1 gives a good indication of why early users wanted to continue to increase the accelerating voltage to gain display brightness. The problem that is encountered is that the beam stiffness goes up as the accelerating voltage is increased. For electrostatic systems, it is inversely proportional to the accelerating voltage and for magnetic systems it is inversely proportional to the square root of the accelerating voltage. It is obvious that it is not quite as severe a problem for magnetic deflection systems as for electrostatic systems.

The solution to this dilemma is to accelerate the beam to the required high voltage after the deflection has occurred (this is called post-deflection acceleration or PDA). This will conserve the power in the deflecting system and give the velocity required for the display brightness. Methods for achieving this were proposed as early as 1920.

Second-acceleration schemes were suggested on several occasions: in 1918 by WFG Swann, in 1920 by W. Rogowski, and in 1923 by A. B. Wood. The first reference to post acceleration being used in a tube was reported in 1928 by E. Sommerfeld.

These first attempts were to place a metal mesh parallel to, and slightly behind, the screen. A positive accelerating field was applied between the mesh and the screen. Later examples of this method are discussed by F. K. Harris (1934) of the U. S. and H. Graupner (1934) in Germany.

The principle difficulties with these tubes were the spot enlargement due to the field penetration through the mesh apertures and the secondary electrons from the mesh which were also accelerated to this positive high voltage and produced a second image. This image is especially apparent as a smaller ghost image as the beam is scanned away from the center of the display area. Because of these problems, this technique never caught on.

Development of Band-type PDA Schemes

Obviously other techniques were needed and the use of planar fields instead of the metallic mesh were considered. Rogowski and Thielen (1939) investigated electrostatic accelerating fields and found them to work satisfactorily. They found that the voltage ratio across the accelerator and its position along the axis are quite important as far as the performance of the system is concerned. Because of the lens action of the accelerator, they were able to reverse the polarity of the deflection at the screen within the range of element position and voltages that they used.

At Phillips, de Gier (1940) reported his work on a single-band accelerator tube and discussed the effects of the accelerator on the sensitivity of the tube and also discussed ways of combating distortions that he encountered.

Pierce (1941) in his paper discussed the change in sensibility (deflecting volts/spot diameter) for PDA schemes using magnetic and electrostatic deflection systems. He concluded that for magnetic deflection systems, since the sensibility is independent of the voltage in the deflection region, the after acceleration only produced increased aberrations, but no change in sensibility. For the electrostatic system, however, the sensibility is proportional to the square root of the voltage and is improved by use of after acceleration but only because the voltage in the deflection system is reduced. As he points out, if deflection compression occurs, deflection defocusing is worse for the same scan in these systems and, in addition, any aberrations from the after-acceleration system that are present must be considered.

A considerable amount of work was done during World War II especially for radar displays. This work was classified, however, and not regularly reported on at the time. The improvements were noted by Christaldi (1945, p. 373) of DuMont:

"Much progress has been made recently in both techniques and designs of cathode-ray tubes and circuits. Both brightness and resolution of the fluorescent spot have been improved. New intensifier-type tubes have been developed for high accelerating potentials with high deflection sensitivity, considerably extending the range of visual observation and photographic recording of cathode-ray traces. It is expected that the improved cathode-ray tubes and techniques which have been developed during

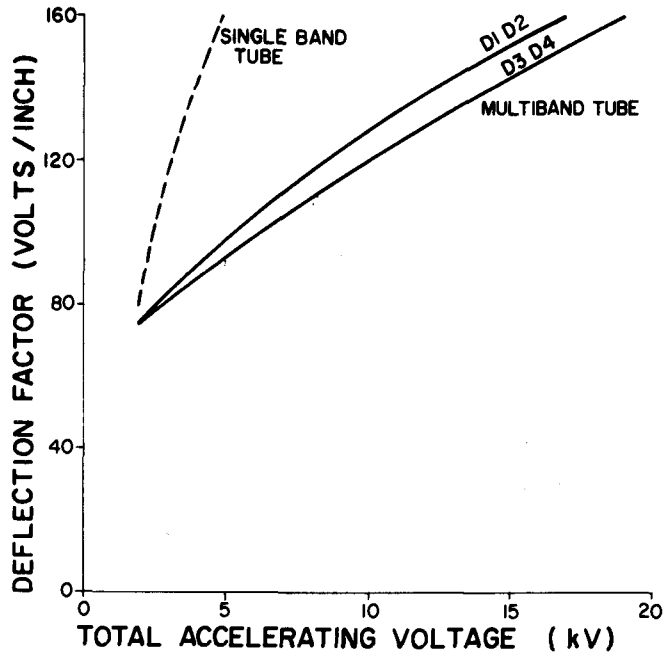


FIG. 2

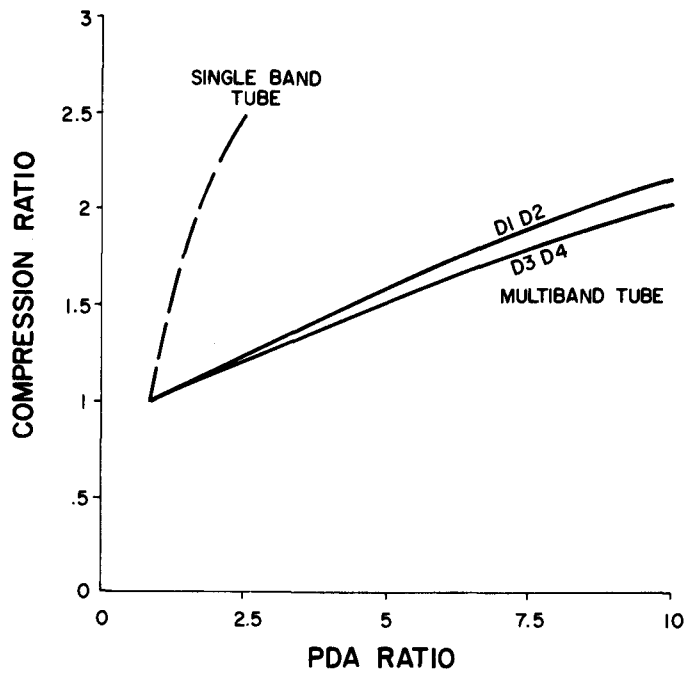


FIG. 3

COMPARISON OF SINGLE AND MULTIBAND TUBE DEFLECTION PERFORMANCE WITH PDA VOLTAGE

the last few years, many of which have not yet been publically described, will be applied to laboratory and production equipment as well as to television transmission and reception."

An attempt was made by MIT to summarize the wartime work in their Radiation Laboratory Series in which volume 22 on Cathode Ray Tube Displays, edited by Soller, Starr, and Valley, Jr. (1948), discussed tube performance especially as related to the user and equipment designer.

Lempert and Feldt (1946) of Dumont give us a first reference to the extension of the band principle to several bands (a multiband tube). They proceeded to apply the post acceleration in several steps. This gave them a larger useful scan area at higher PDA ratios than had been attained previously.

A comparison of their multiband to a single-band tube is given in Figure 2. Figure 3 is the data reinterpreted into another format which is more familiar to the author.

The problems of scan compression and distortion at high PDA ratios were the limiting factors for the tube built during the late 1940's. W. G. White (1949) in England suggested moving the high voltage electrode to the back of the phosphor and accelerate the electrons at the last instant. He didn't seem to understand that the field from this electrode would penetrate back into the tube and affect the scan in somewhat the same manner any band would. The problems associated with his idea were immediately pointed out by his countryman, Allard (1950), who described a noncompressing PDA

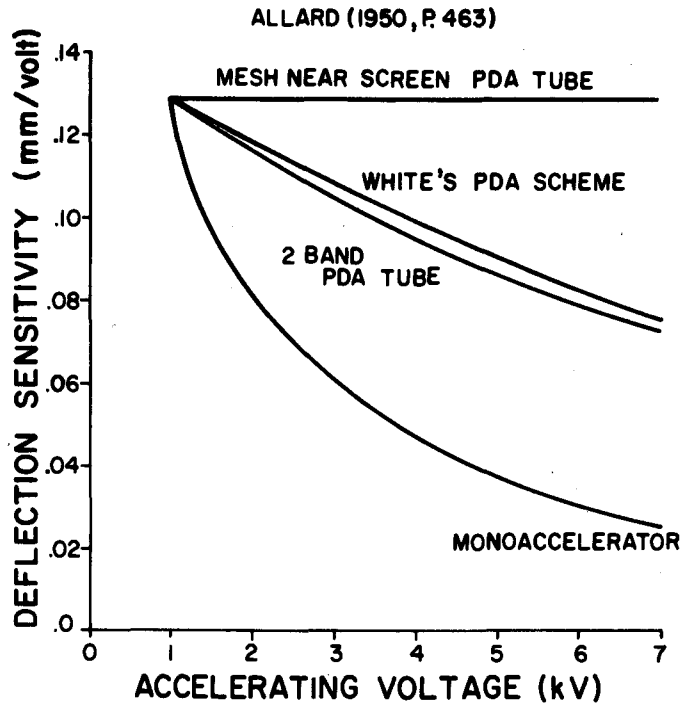


FIG. 4

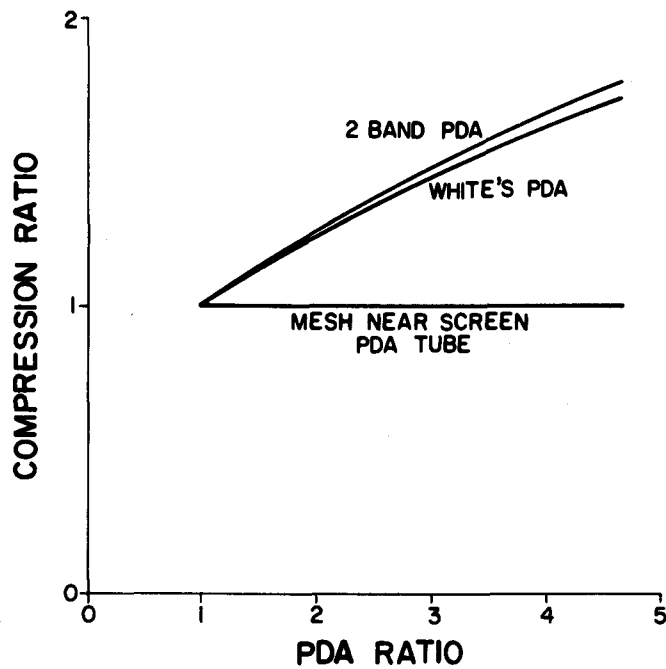


FIG. 5

COMPARISON OF SCAN COMPRESSION PERFORMANCE FOR VARIOUS PDA TUBE TYPES.

scheme that used a mesh near the screen. Allard concluded that although the system had no compression, as shown in Figures 4 and 5, it suffered severely from secondary electrons from the mesh which reduced the display contrast and gave a ghost spot which in turn again reduced the resolution somewhat. He concluded that these disadvantages outweighed the advantages "thus rendering its practical usefulness of small value"; Allard (1950, p. 463). He had reconfirmed the results of the work done in the early 1930's.

This work stirred considerable interest and attempts were made to provide a collector for the secondary electrons to eliminate the ghost spot. Several schemes were proposed and patented in the U. S. Smith (1950), at General Electric, proposed using a collector ring near the mesh which would run slightly positive with respect to the mesh and, therefore, collect the electrons; Hoagland (1951), at DuMont, used a double mesh with the collector mesh at a slight positive potential. But even these improvements didn't make this type of tube popular. Obviously, the improvements weren't good enough.

Pattern distortion (geometry) and edge defocus on the multiband PDA tubes led to extensive work in improvement of monoaccelerators. At DuMont, Grossbohlen and Hoagland (1953) reported that with better production techniques, enabling them to hold tighter spacing and tolerances on the deflection plates, they had been able to design a 6 kilovolt monoaccelerator that competed in brightness and sensitivity with their 10.5 kilovolt PDA tube (7:1 PDA ratio); it was better with respect to the geometry of the display and had less edge defocus. The disadvantage was a 33 percent increase in input capacitance which they

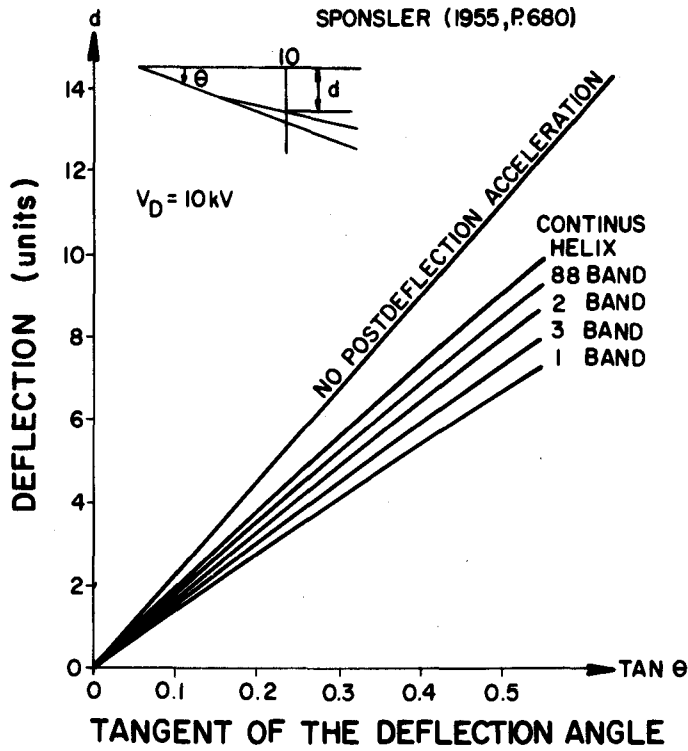


FIG. 6
COMPARISON OF DEFLECTION vs.
DEFLECTION ANGLE TANGENT FOR
BAND & HELIX TYPE PDA TUBE.

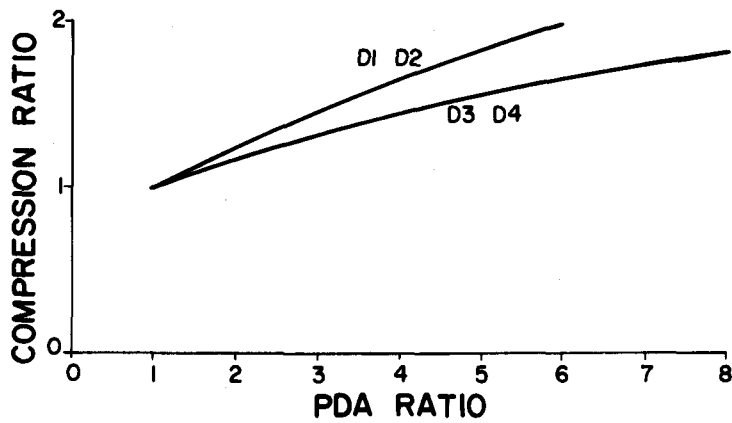


FIG. 7
COMPRESSION RATIO vs. PDA RATIO
FOR HELIX PDA TUBE

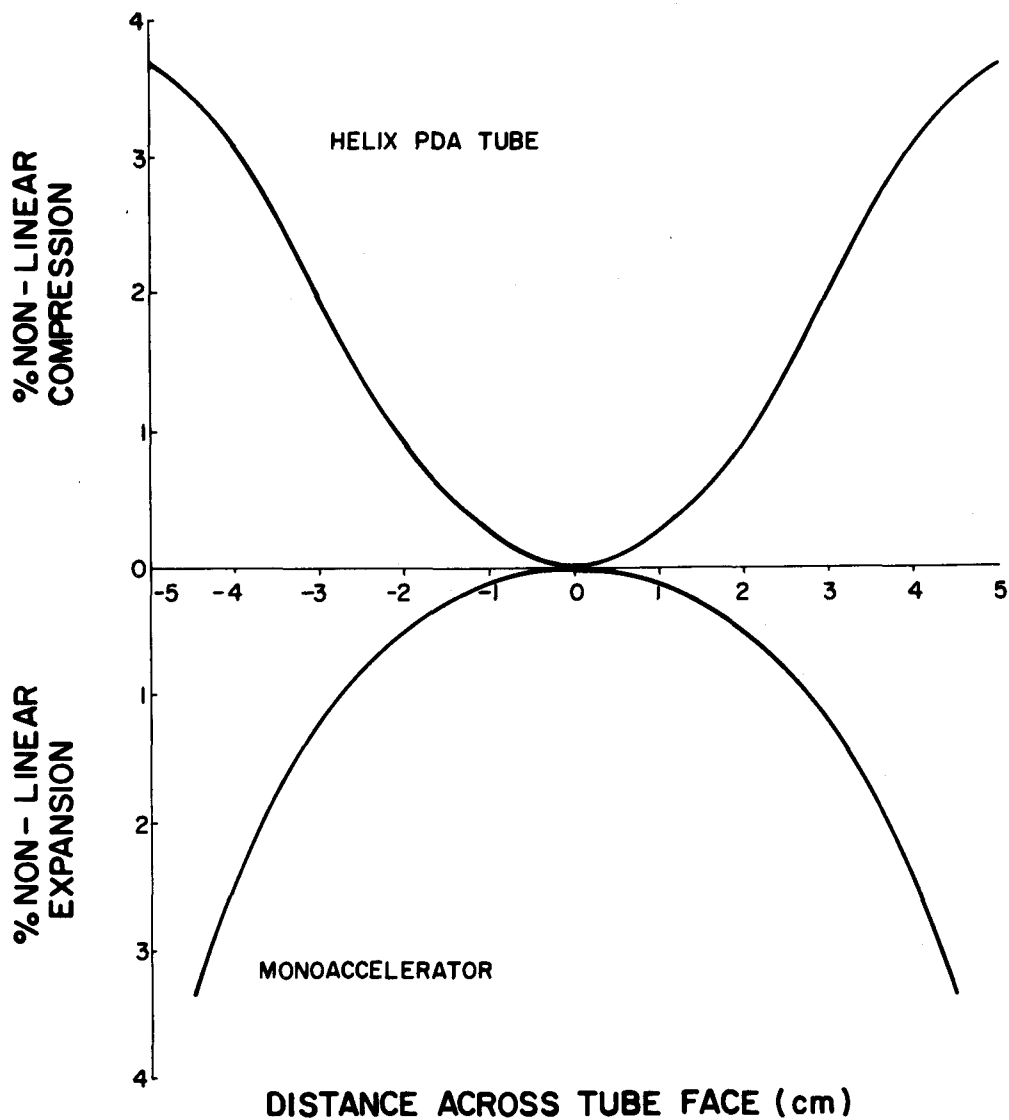
argued was not a major problem for them.

Development of Helix-type PDA Schemes

Proponents of PDA systems continued to look for improvements for their systems. It was obvious from the work of Lempert and Feldt (1946) that the use of multiple bands softened the lens effect and reduced the scan compression. Practical constructional considerations limited the number of bands to about five. An early proposal by Schwartz (1933) of using a continuous resistive helix applied to the full length of the bulb was followed up. This technique provided a very soft lens since many bands (70 to 90) were used. The first commercial tubes of this type were available from Tektronix in 1954. An evaluation of the relative merits of multiband and helix PDA schemes was done by Sponsler (1955) at MIT by plotting electron trajectories in a tube analog. He used an electrolytic tank to set the field conditions and had a computer follow the electron trajectory through the field. Figure 6 shows the advantage of the continuous helix over other band systems.

Sponsler (1955) also claimed that the display linearity should be better for the helix because there was less curvature $\left(\frac{d \text{ defl}}{d \tan \theta}\right)$ shown for that system. Figure 8 depicts the nonlinearity for the deflection factor measured across the face of the CRT for both a monoaccelerator and a helix PDA tube. The nonlinear expansion of the mono is due principally to the flat face of the CRT.

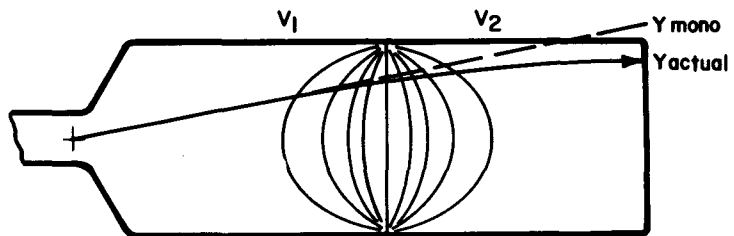
This new PDA scheme quickly gained acceptance and within three to four years most tube manufacturers here and abroad were producing



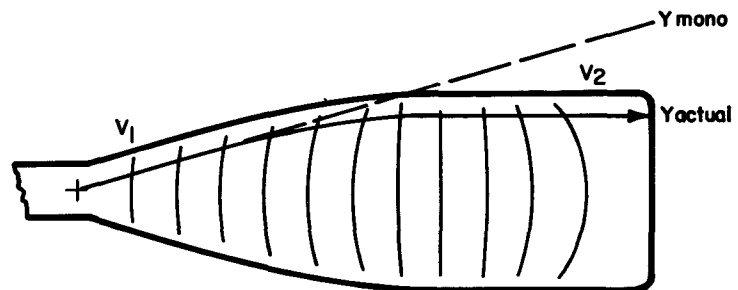
DISTANCE ACROSS TUBE FACE (cm)
FIG. 8
COMPARISON OF LINEARITY CHARACTERISTICS

tubes of this type. Although the helix PDA gave improved performance, through less scan compression and less geometrical distortion, it did not eliminate the compression entirely. Efforts were continued to eliminate this undesirable effect.

At DuMont, Bramley (1956) patented a special form of a single-band tube that shaped the field in a way to be noncompressing through PDA ratios of 5:1. Schleisinger (1956), then at Motorola, evaluated the use of mesh-type PDA schemes at 10:1 PDA ratio with a biased mesh for ghost suppression as part of his work on electrostatic TV tubes. He reported that the system operated satisfactorily. Frenkel (1957), then at Tektronix, patented a PDA tube that employed a combination magnetic and electrostatic lens in the PDA region. This lens projected the image to be displayed on the screen. He claimed that the geometric distortions due to the electrostatic lens were cancelled by opposite distortions in the magnetic lens. The display size was reported to be independent of the deflection factor of the gun. Owren (1959) at Abtronics patented a PDA tube that uses several meshes to form a spherical field that magnified the display. Dolan and Niklas (1960) at Rauland investigated the use of a mesh at the mid-potential of a two-element (band-type) PDA lens to convert the lens from a convergent to a divergent lens. Although the system worked, they were dissatisfied because of the high current loss in the mesh and the defocusing of the spot due to the lenslets at each mesh aperture. Law, Davne, and Ramberg (1960), at RCA, made use of a spherical mesh protruding into the high voltage PDA field to investigate an



SINGLE BAND PDA



HELIX PDA

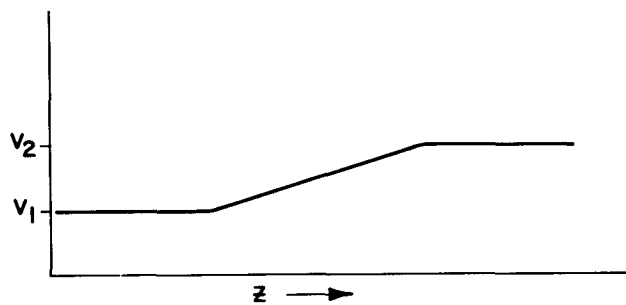


FIG. 9

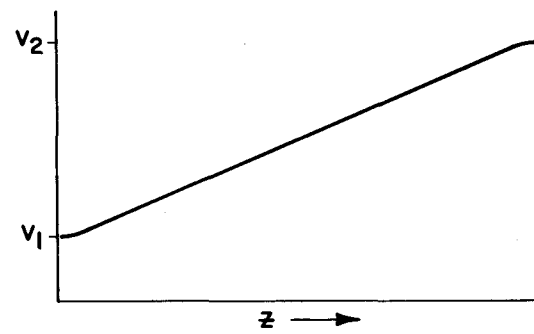


FIG. 10

enhanced scan (magnified display) TV tube. The mesh was operated considerably below the voltage of the electron beam to increase the divergent action of the system. They reported that the tube operated satisfactorily while the required scanning power was reduced considerably, the brightness loss due to the mesh intercept was a problem.

In each case, for the work just described, the solutions arrived at created about as many mechanical or electrical problems as they solved. As far as the author knows, none of the above-mentioned developments were widely received or used.

The Problem Defined

As has been discussed, the general problem with conventional band or helix PDA schemes is the scan compression resulting from the lens action of the accelerating field as shown in Figures 9 and 10.

This problem can be minimized or eliminated if the accelerating field were normal to the electron trajectory all during its transit time from the deflection system to the fluorescent screen. This is discussed by DeGeir (1940) in his work on post deflection acceleration. He, however, "simplified" his system to the single-band (2 voltage) case discussed above, because "In practice it has been found that such a complicated structure is unnecessary; instead . . . two broad coatings can be used . . ."; deGeir (1940, p. 247). His simplification cost him a reduction in deflection sensitivity to one-half the original value (2:1 compression factor) at the voltages he was using. This was

a better compromise than his other alternative, however, since operating the tube as a high voltage monoaccelerator would have resulted in a deflection sensitivity reduction to 1/5 the original value.

Therefore, his net gain was a factor of 2.5 times in deflection sensitivity plus a gain of 10 times in light output at the screen.

Even with the attendant problems of scan compression, the band system along with the helix improvement served as the mainstay for the oscillographic CRT for 20 years until the introduction of transistorized circuits into the oscilloscope field changed the basic tube requirements.

The transistor, with its high current and low voltage characteristics, was not amenable for use as the output drive amplifier for the CRT deflection plates. Several then popular instruments at Tektronix required 28V total signal for a 4 cm 30 MHz display or 60V total signal for a 6 cm 15 MHz display. In addition, allowance must be made for things such as linear signal positioning, which further complicates the output amplifier design.

The transistor requirement called for a tube of lower deflection factor and increased scan size plus an increase in writing speed and luminance to match the increased bandwidth requirements. The final evaluation of the system requirements led to the development of the mesh-type tube.

The basis for the operation of the tube as pointed out by deGeir is to produce an accelerating field that is always normal to the electron trajectory. A system that meets these conditions is that of

a spherical system in which the electrons are emitted from the surface of one sphere into the electrical field between that sphere and a larger sphere. This system needs to be examined in more detail.

II. THEORY OF OPERATION OF THIS NONCOMPRESSING METHOD

A Simple Model

Consider an isolated spherical conductor having a charge on it about which it is necessary to find the electric field. The two given boundary conditions are, (1) the surface of the sphere is an equipotential surface, and (2) the total charge on the sphere is Q . These will be used to help find a potential field that satisfies Laplace's equation.

$$\nabla^2 V = 0$$

Since the system is spherical, spherical coordinates will be used as shown in Figure 11. Laplace's equation in spherical coordinates is then

$$\nabla^2 V = \frac{\partial^2 V}{\partial r^2} + \frac{1}{r^2} \frac{\partial^2 V}{\partial \theta^2} + \frac{1}{r^2 \sin^2 \theta} \frac{\partial^2 V}{\partial \phi^2} + \frac{2}{r} \frac{\partial V}{\partial r} + \frac{\cot \theta}{r^2} \frac{\partial V}{\partial \theta} = 0$$

Since the sphere is isolated in space, the problem can be considerably simplified because of symmetry. This is because of the isolation; there is no other object to which to reference θ and ϕ , therefore, only r is a defined direction. The electric potential V must then be the same for all values of θ and ϕ which reduces Laplace's equation to:

$$\nabla^2 V = \frac{\partial^2 V}{\partial r^2} + \frac{2}{r} \frac{\partial V}{\partial r} = 0$$

Laplace's equation in this form has the solution

$$V = \frac{a}{r} + b.$$

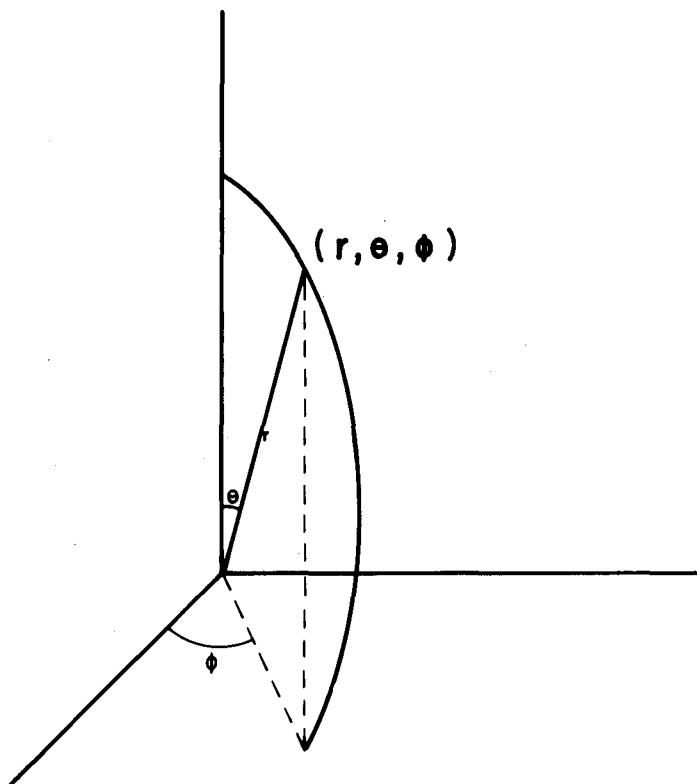


FIG. II

DEFINITION OF COORDINATE DIRECTIONS
FOR SPHERICAL COORDINATE SYSTEM

To evaluate the arbitrary constants, assume that at a great distance from the sphere, $r = \infty$, the field is not perturbed by the charge on the sphere, $V = 0$; this substitution gives $b = 0$ and the equation reduces to

$$V = \frac{a}{r}$$

The remaining constant, a , will be evaluated in terms of the charge on the sphere.

For a sphere of radius r_0 , the charge must be distributed symmetrically over the surface and the charge per unit area σ is

$$\sigma = \frac{Q}{4 \pi r_0^2} \quad \frac{\text{coulombs}}{\text{meter}^2} .$$

Since the charge density is a function of the electric field strength and the permittivity, $\sigma = \epsilon E$, the electric field strength can be determined viz,

$$E = \frac{Q}{4 \pi \epsilon r_0^2} \quad \frac{\text{volts}}{\text{meter}} .$$

Again, because the potential gradient is only radial, the electric field strength at any point is found to be

$$E = - \frac{\partial V}{\partial r} = \frac{a}{r^2} \quad \frac{\text{volts}}{\text{meter}} .$$

Equating the last two expressions gives

$$\frac{a}{r_0^2} = \frac{Q}{4 \pi \epsilon r_0^2}$$

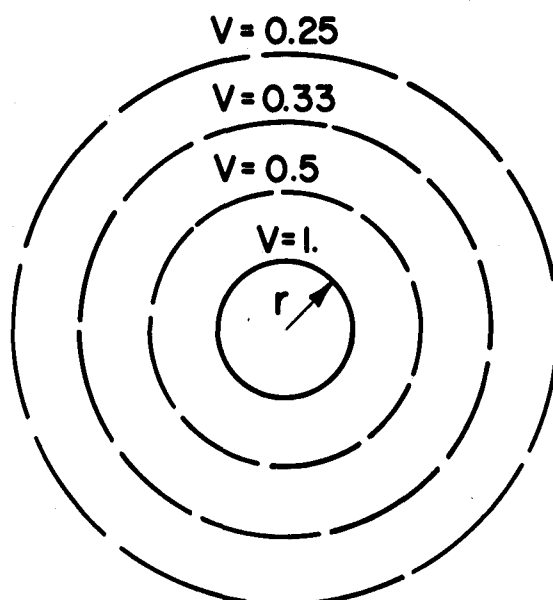


FIG. 12

EQUIPOTENTIALS AROUND A SPHERE

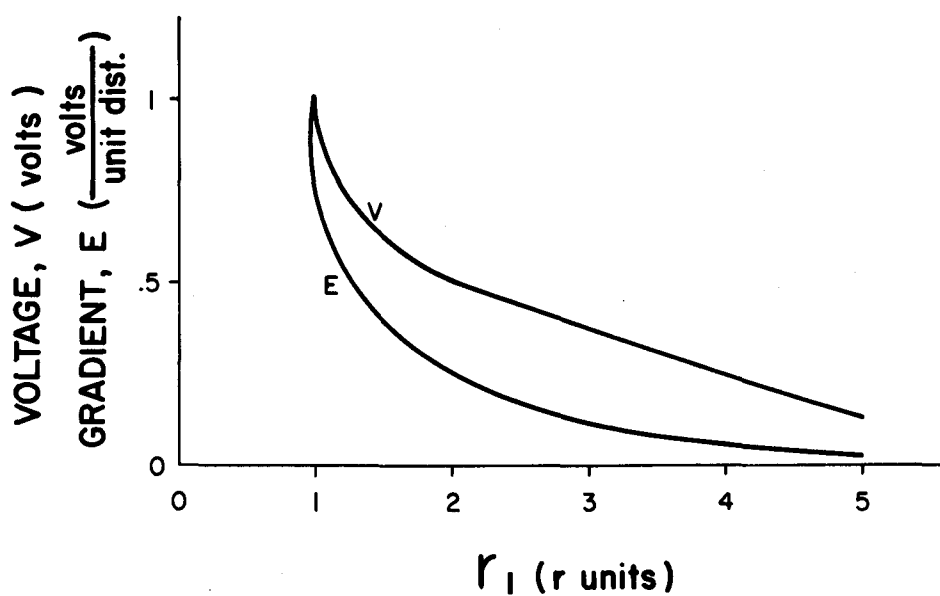


FIG. 13

POTENTIAL & POTENTIAL GRADIENT
AROUND A SPHERE

from which

$$a = \frac{Q}{4 \pi \epsilon} .$$

Substituting back into the original equation to find the potential about the sphere

$$V = \frac{Q}{4 \pi \epsilon r} \quad \text{volts.}$$

In addition, the potential gradient has been determined to be

$$E = \frac{a}{r^2} = \frac{Q}{4 \pi \epsilon r^2} \quad \frac{\text{volts}}{\text{meter}} .$$

It has been shown then that the potential distribution achieved by the spherical system is inversely proportional to the radius and, as was discussed, is only a function of the radius.

Figure 12 shows equipotentials in the region of the sphere and Figure 13 shows the potential distribution and the electric field strength as a function of the distance (in radii) from the sphere.

It is seen that electrons injected normally into this system would travel radially, or without deflection, as was suggested. This particular system will, however, decelerate the electrons because the voltage decreases as the radius increases. The model discussed should then be modified to provide an accelerating field.

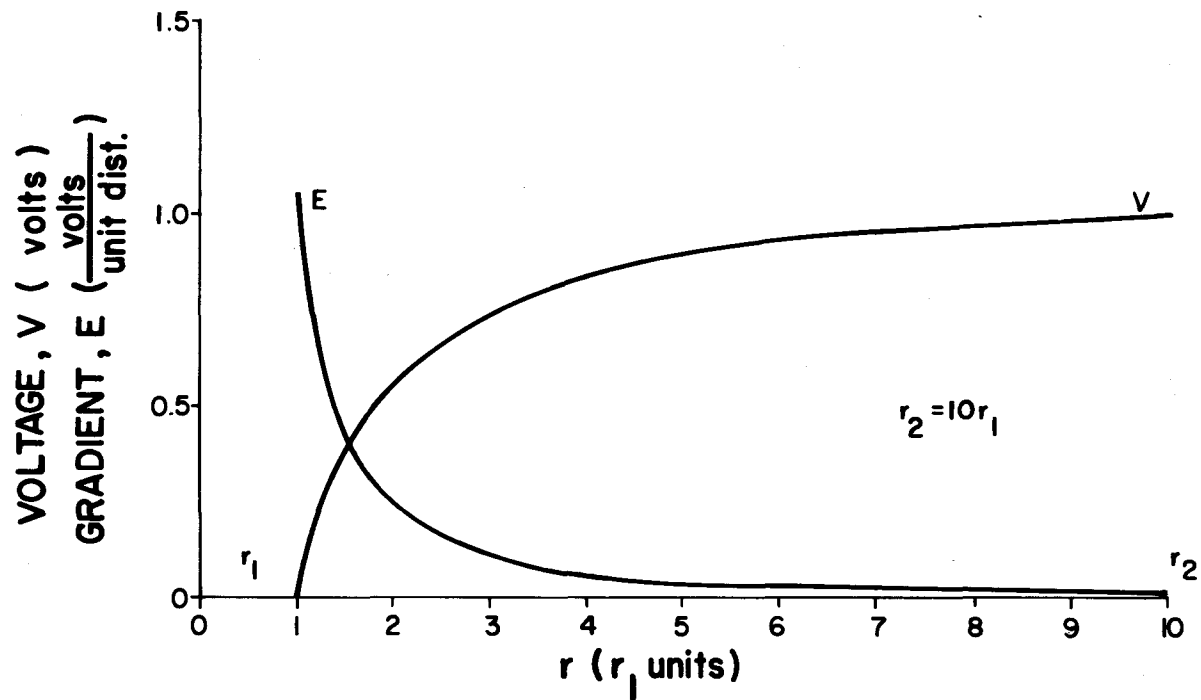


FIG. 14
POTENTIAL & POTENTIAL GRADIENT FOR AN
ACCELERATING FIELD BETWEEN TWO SPHERES.

The Model Refined

In the case just discussed, any equipotential of Figure 12 could be replaced by spherical conductor which would be maintained at the potential of the surface that it replaced and not disturb either the potential distribution or the gradient.

The voltage between these two spheres (r_1 and r_2) would be

$$\begin{aligned}
 V_{12} &= \int_{r_1}^{r_2} E dr = \int_{r_1}^{r_2} \frac{Q}{4 \pi \epsilon r^2} dr \\
 &= \frac{-1}{4 \pi \epsilon} \left(\frac{Q}{r_2} - \frac{Q}{r_1} \right) = \frac{1}{4 \pi \epsilon} \left(\frac{Q}{r_1} - \frac{Q}{r_2} \right) \\
 &= \frac{Q}{4 \pi \epsilon} \left(\frac{r_2 - r_1}{r_1 r_2} \right) = \frac{Q (r_2 - r_1)}{4 \pi \epsilon r_1 r_2} \quad \text{volts.}
 \end{aligned}$$

There has been no restriction placed on the sign of Q and, if it is allowed to be negative, then $V_2 > V_1$ or, for the electrons, an accelerating field is present.

The system would then be described by the equations

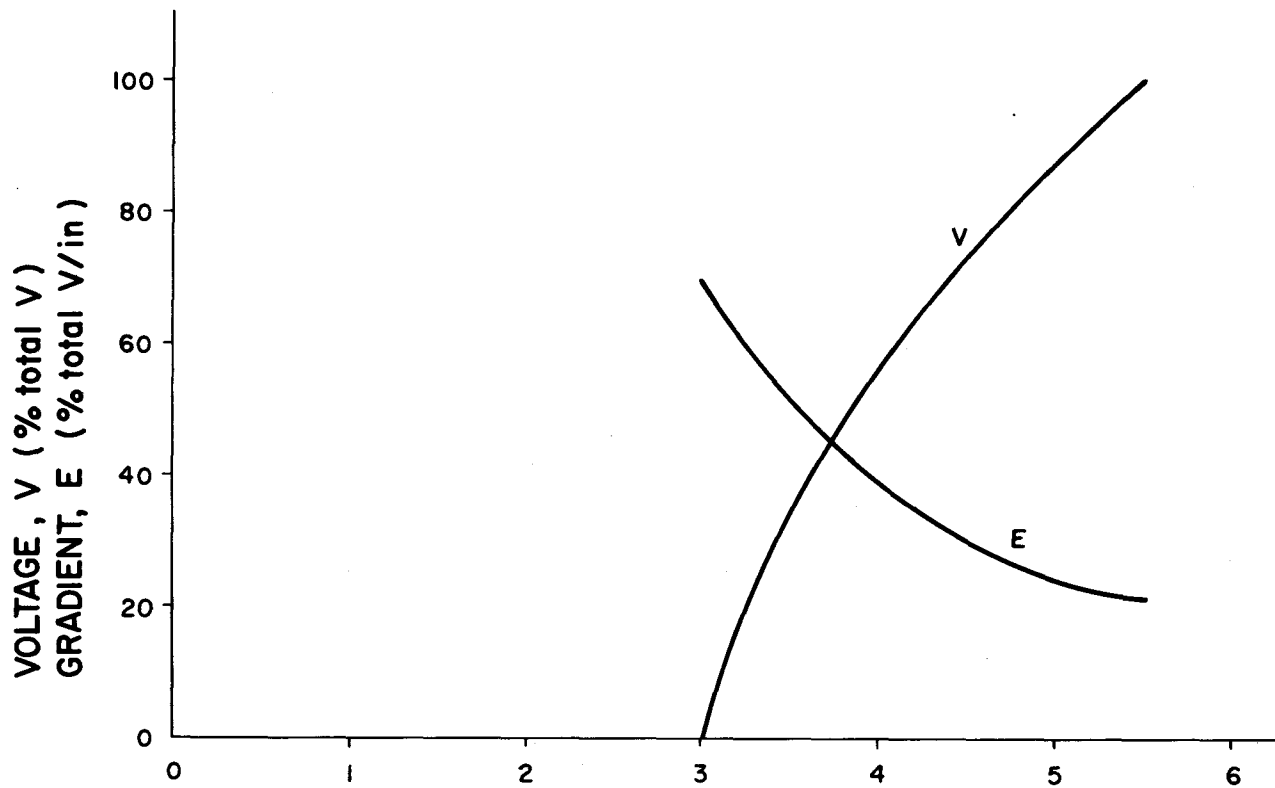
$$V = \frac{Q (r_2 - r_1)}{4 \pi \epsilon r_1 r_2} \quad \text{volts}$$

and

$$E = \frac{-Q}{4 \pi \epsilon r_2^2} \quad \frac{\text{volts}}{\text{meter}}$$

This is graphically shown in Figure 14.

This system would now accelerate the electrons radially as was originally proposed. The system is conceptually simple and mathematically straightforward. It is now necessary to apply the concepts of the system to a workable device.



RADIAL DISTANCE FROM CENTER OF CURVATURE OF THE SYSTEM (inches)

FIG. 15

VOLTAGE & GRADIENT BETWEEN TWO SPHERES

III. PRACTICAL CONSIDERATIONS

Having determined, then, the voltage distribution required in the accelerating region that only acts on the electrons in the deflected direction and that produces no radial force, which would produce scan compression, it is necessary to consider the application of this idea to a practical system.

Application to a Closed System

Using the equations developed in the last section and assuming radii for the two spheres of $r_1 = 3''$ and $r_2 = 5-1/2''$, the voltage and voltage gradient can be determined and are shown in Figure 15. This same voltage distribution and gradient can be achieved in a closed system, such as a conical section taken from the spherical system in which the center of the sphere is the point of the cone. In order to achieve this electrostatic field in the closed space chosen, it is necessary to impose the calculated voltage distribution on the boundaries enclosing that space.

The boundary conditions chosen obviously resemble a cathode-ray tube and Figure 16 shows the distribution of equipotentials in a bulb, when the boundary voltage distribution just discussed was applied. These plots were made in an electrolytic tank. Since the system shown does not exactly conform to the ideal system as it was developed earlier, the voltage and gradient will be a function of the region that is chosen to evaluate it. Figure 17 shows the voltage

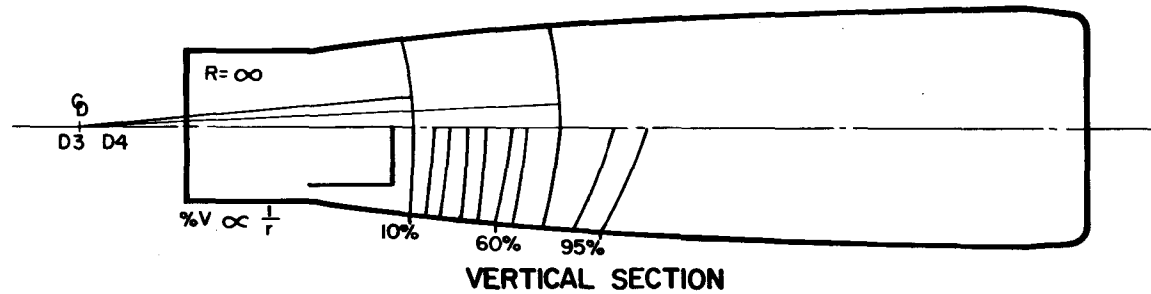
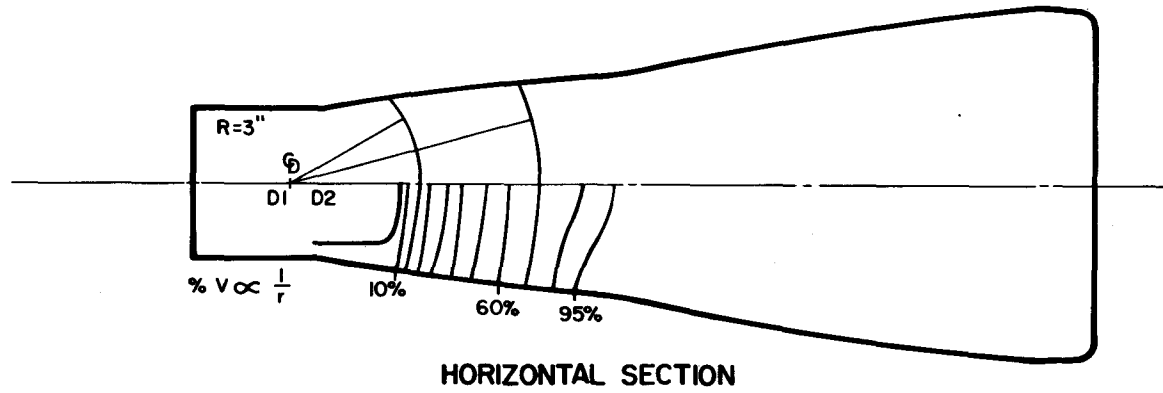


FIG. 16
ELECTROLYTIC TANK PLOTS SHOWING
DISTRIBUTION OF EQUIPOTENTIALS
IN THE BULB.

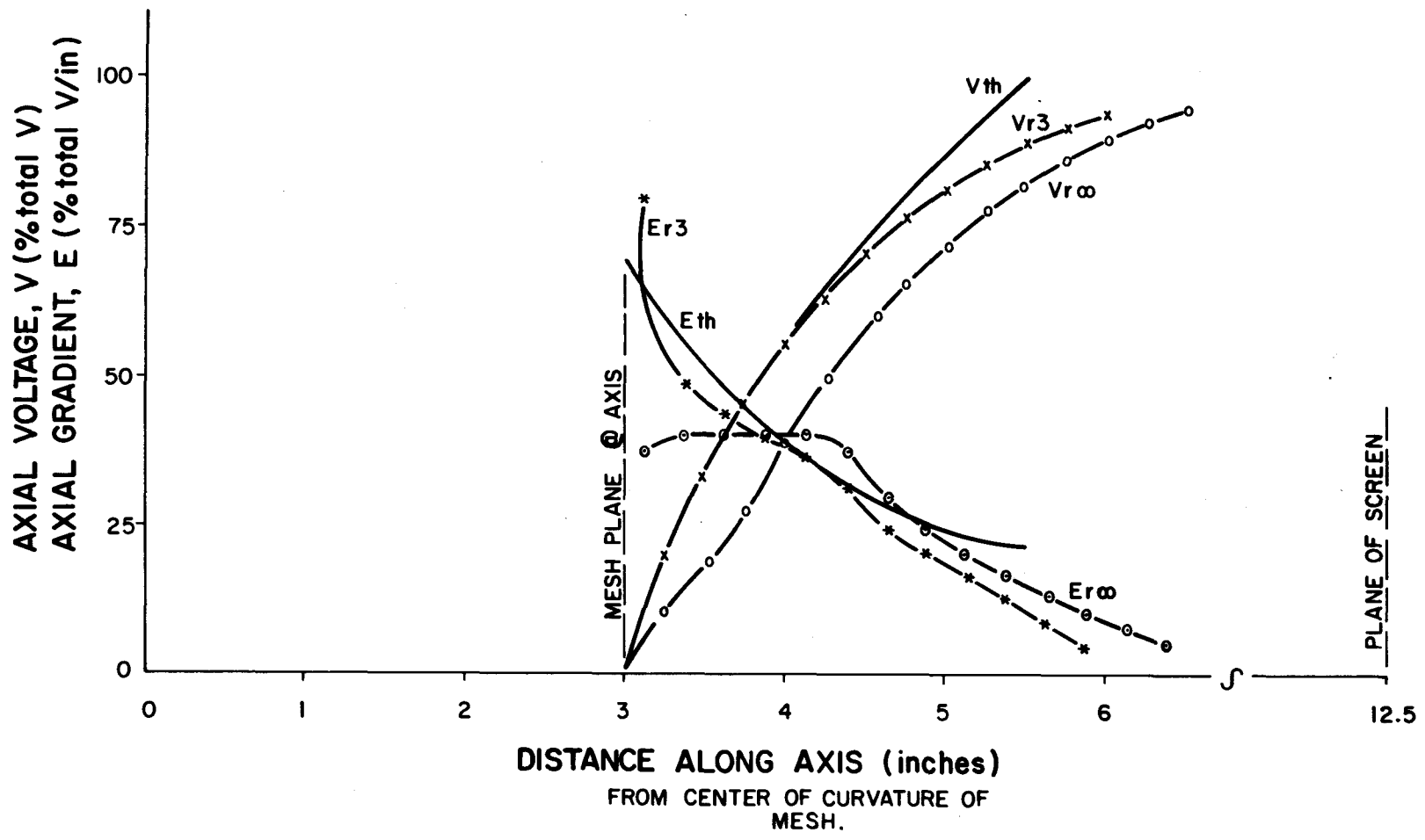


FIG. 17

and the gradient along the Z axis for the two conditions shown in Figure 16; in addition, the theoretical curve from Figure 15 is included for comparison. This evaluation in two planes through the bulb is still a somewhat simplified picture, and it should be noted that since the axis shown is common to both sections, the potential along that axis must be the same for both cases. The actual voltage and gradient achieved in the bulb would then be the average of the two curves shown. As can be seen, the voltage does not reach the full value at the point predicted because there is no sphere or other conducting surface to terminate the field there. The field is allowed to establish its own equilibrium as can be seen in Figure 16. In general, the axial voltage and axial gradient fall within 10 to 15 percent of the calculated values.

System Restrictions

Considering the design from the point of view of the concentric spherical system, it would be advantageous to consider the center of deflection; i.e., that hypothetical point in the deflection structure which is the rearward projection of the beam to its "source" (as shown in Figure 18), as the center of the spherical system, $r = 0$.

For the type of CRT that would be considered to meet the given requirements, this is not the case. There are two sets of deflection plates (for horizontal and vertical deflection) and these are separated along the tube axis by several inches. Since both center of deflections cannot act as the center of the acceleration system, one or the

other or some judicious compromise between the two must be made. Considering several factors, including the design of the field-forming electrode, it was decided to favor the center of deflection of the DID2 deflection system as the center of curvature of the PDA region.

Another problem area is the choice of the fabrication technique for the field-forming electrode. This electrode, which serves to form the field to the spherical shape desired, can be constructed in either of two ways. Electroformed mesh would be very amenable to forming in the spherical shape required, but would have the disadvantage of having only 40 to 50 percent electron transmission thru the mesh and be quite fragile in the mesh pitch range required (500 to 1,000 lines/inch). The other technique is to use a wound tungsten wire grid which would have higher electron transmission - 70 to 80 percent - at the pitch required, and it would be less fragile because of the material used; but it could only be formed to a cylindrical, not spherical, shape because of the wires under tension. For this case, it was decided that the higher electron transmission was the more important factor. In addition, since the centers of deflection are separated by several inches, the field curvature required for the D3D4 system was less than that required for the DID2 system. Examination of Figure 16 again shows that, for the flat plane of the mesh, the curvature of the field substantially corresponds to that required as shown by the arcs of circles of the appropriate radii drawn in the upper half of the bulb. For these several reasons, the

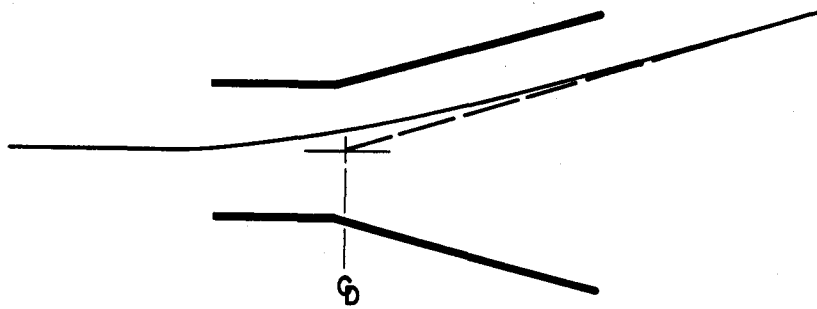


FIG. 18

DEPICTION OF CENTER OF DEFLECTION
FOR A PAIR OF DEFLECTION PLATES

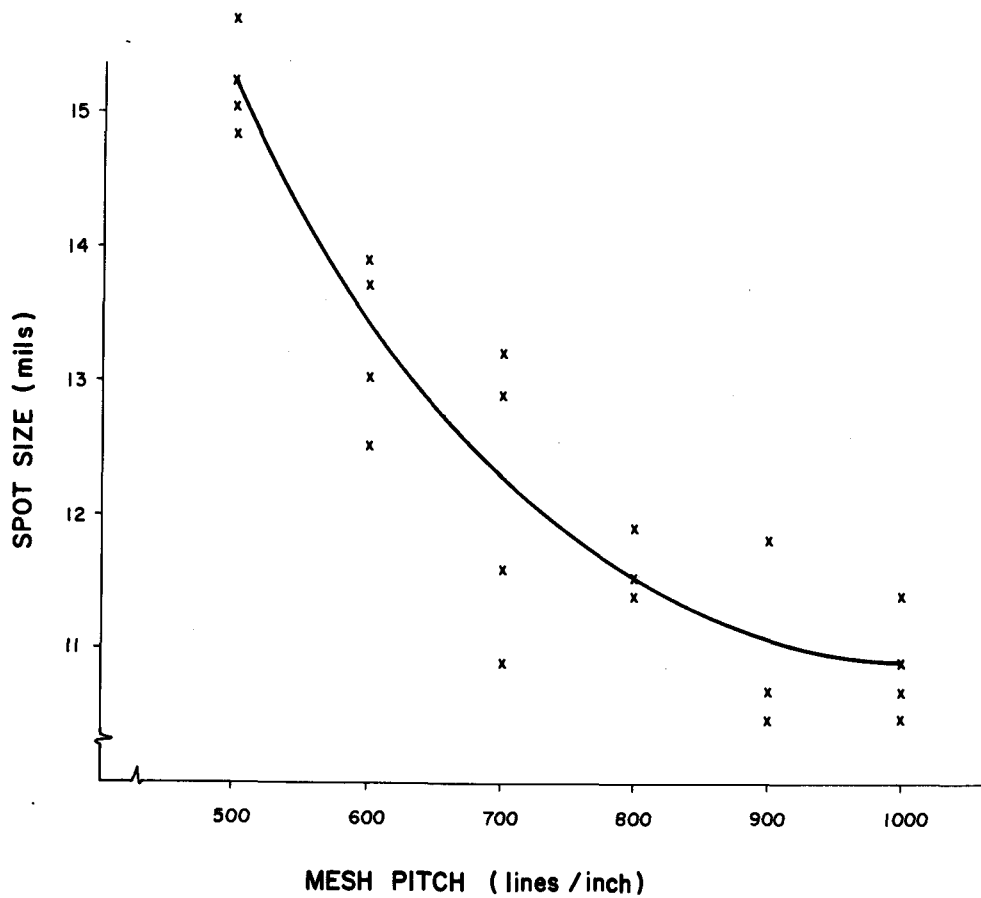


FIG. 19
SPOT SIZE vs. MESH PITCH

frame grid technique was chosen.

A third major restriction was due to the allowable shape of the envelope of tube. It was a requirement that the concept of a round CRT with a rectangular display area be abandoned in order to minimize the unused front panel space on the instrument. This forced the bulb to a rectangular shape. The consequence of this was that the accelerator electrode (a short helix) that serves to fix the boundary conditions on the accelerating field would be difficult to apply in the region near the screen, and, furthermore, would not have rotational symmetry. This would force additional complication in the application of this electrode to maintain any given equipotential thru a 360° rotation at any point along the Z-axis of the tube. It was necessary, therefore, to keep the electrode in the round or near round portion of the bulb. As was discussed earlier, this restriction gives sufficient conformance with the calculated values to be acceptable. This is, of course, shown by Figures 16 and 17 and the discussion that was given there.

It is appropriate at this point to discuss the degradation of the trace width due to the mesh pitch. The voltage gradient, E , at the mesh will be on the order of 8 to 12 kilovolts per inch, and this high gradient will serve to degrade the trace width as the equipotentials penetrate through the windings of the mesh. As the mesh wires are brought closer together, any given equipotential line will have its curvature reduced. This reduction in curvature will

serve to increase the focal length of that lenslet. This increase in focal length will reduce the measured degradation of the trace. Figure 19 shows the spot degradation due to the mesh pitch and clearly indicates that a 1,000 line per inch system should be used.

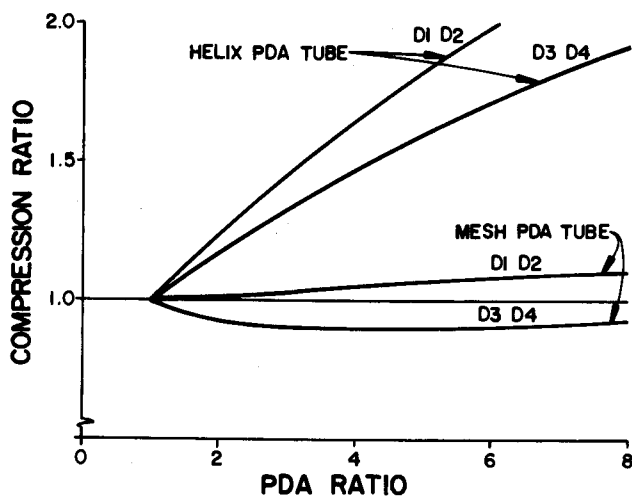


FIG. 20
 COMPARISON OF SCAN COMPRESSION FACTORS
 FOR STD. HELIX & MESH TYPE PDA TUBE.

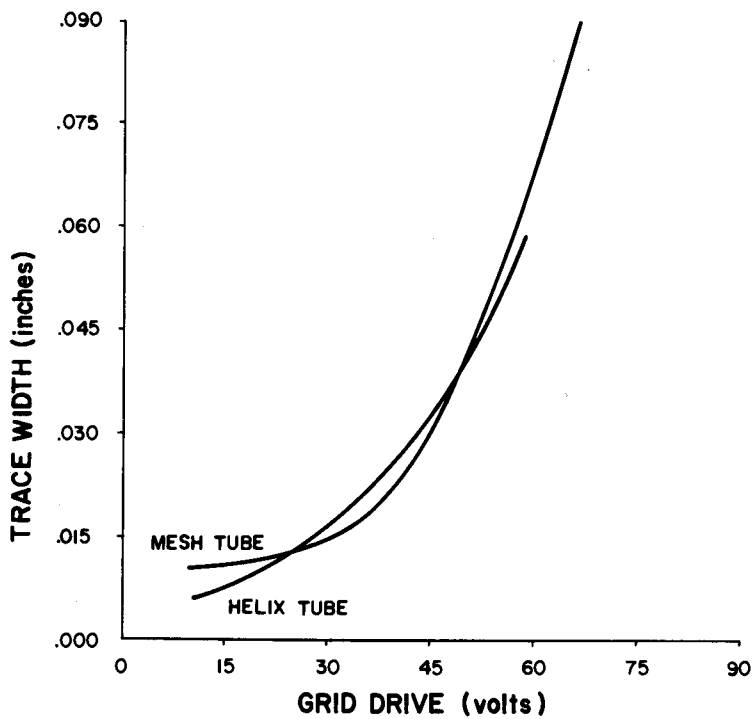


FIG. 21
 TRACE WIDTH COMPARISON FOR HELIX
 & MESH PDA TUBE.

IV. EVALUATION OF THE FINAL SYSTEM

Having taken into account the compromises just discussed, it is necessary to compare the performance of this new system against available systems.

Performance Comparisons

Figure 20 compares the scan compression of this new mesh PDA system to the standard helix system. It is obvious that the system performs in the required manner. There is less than a 10 percent change in the scan thru the PDA ratio examined as compared to a 200 percent change for the standard helix PDA tube. In addition, the slight expansion for the D3D4 (vertical) system can be used to a good advantage in that it helps to further minimize the required driving voltage.

The measured spot size for the two types that are being compared are similar except at the very lowest grid drive. Since the mesh PDA system does not have the spot size reduction due to the scan compression that the helix system does, the design was slightly more difficult. The final result is, however, a minimum spot of 12 mils versus a 10 mil spot for the helix tube. Figure 21 compares the trace width of the two types.

The high gradient at the mesh also affected the overall resolution of the system. Figure 22 depicts the spot deterioration and change in edge resolution versus the PDA ratio. The basic spot size

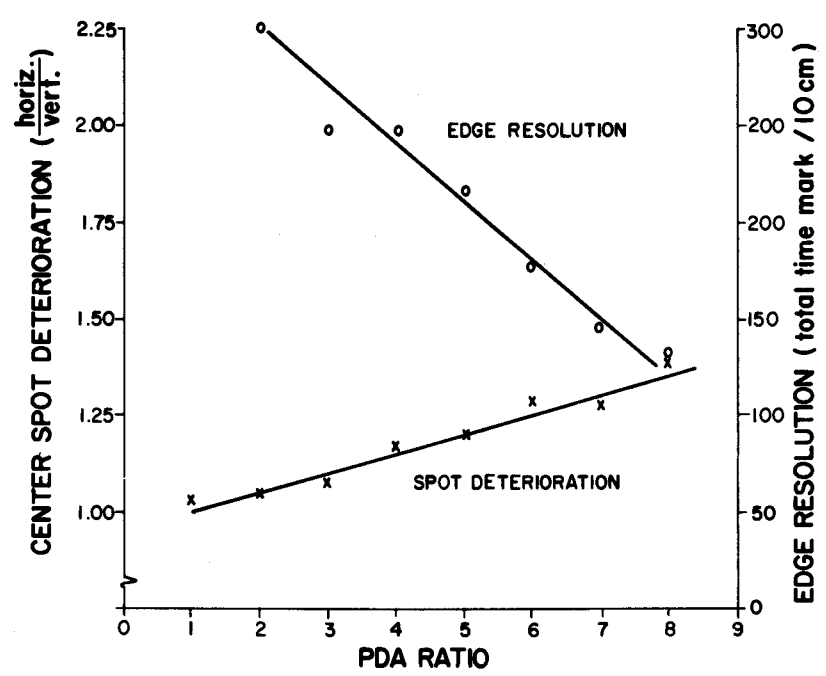


FIG. 22
 DETERIORATION OF RESOLUTION
 vs. PDA RATIO FOR THE MESH PDA TUBE

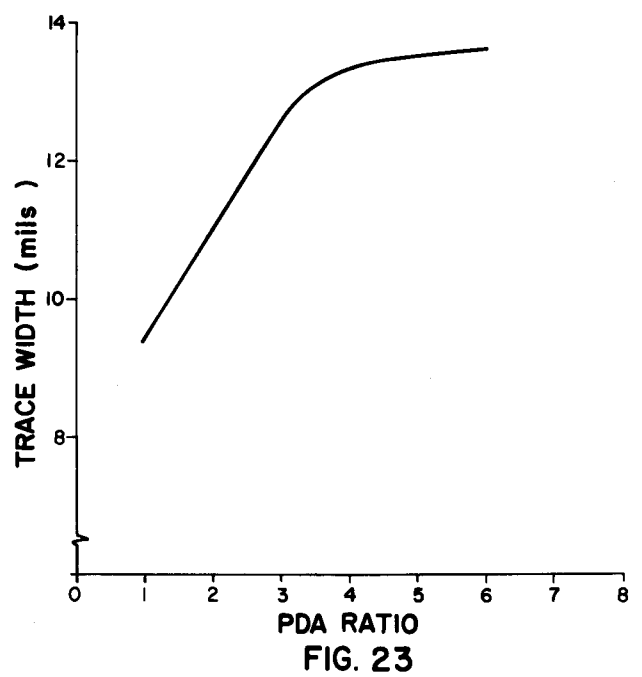


FIG. 23
 CHANGE OF TRACE WIDTH WITH
 PDA RATIO FOR THE MESH PDA TUBE

changed slightly with PDA ratio (see Figure 23). In order to exclude the effect of this change in the evaluation, the ratio of the horizontal trace width to vertical trace height was used as a measure of deterioration. To check the overall or edge resolution capability, a time mark test was used; this display is a comb of equally spaced vertical lines. At a 6:1 PDA ratio, this tube will display 175 total lines compared to slightly less than 100 total lines for the helix system.

Table I. compares the performance of the monoaccelerator and helix tube that have been used for comparison throughout this paper. In addition, an improved helix tube, which was designed at the same time this present work was done, is included. Inspection of the table shows that the mesh tube is superior to the helix tubes in every respect. The normalized deflection factor is considerably reduced for the mesh tube because of the lack of scan compression. Without the spot compression normally encountered, the sensibility has been maintained while the writing speed has been considerably increased.

As has been noted, the photographic writing speed of the mesh system is more than 50 percent faster than the helix system. This is due to fact that the elimination of scan compression has allowed higher voltages to be used throughout the system. The helix tubes run at 10 kilovolts overall voltage, and the mesh tube at 14 kilovolts. The limitation of the voltage used in the system lies in the maximum deflection voltage available and is not a fundamental limit of the CRT

TABLE I. CRT PERFORMANCE COMPARISON

Type	Scan	Normalized Deflection Factor	Maximum Sensibility	Photographic Writing Speed	Writing Speed Index	Information Writing Speed Index
Monoaccelerator	8 cm	5.6 V/cm/kV	490 $\frac{\text{m volts}}{\text{spot dia.}}$	265 $\frac{\text{cm}}{\mu\text{sec}}$	2.0	5.0
Helix PDA (A)	4 cm	4.0 V/cm/kV	165 $\frac{\text{m volts}}{\text{spot dia.}}$	700 $\frac{\text{cm}}{\mu\text{sec}}$	1.0	4.0
Improved Helix PDA (B)	6 cm	3.6 V/cm/kV	180 $\frac{\text{m volts}}{\text{spot dia.}}$	770 $\frac{\text{cm}}{\mu\text{sec}}$	1.2	5.5
Mesh PDA	6 cm	2.4 V/cm/kV	160 $\frac{\text{m volts}}{\text{spot dia.}}$	1075 $\frac{\text{cm}}{\mu\text{sec}}$	1.6	7.5

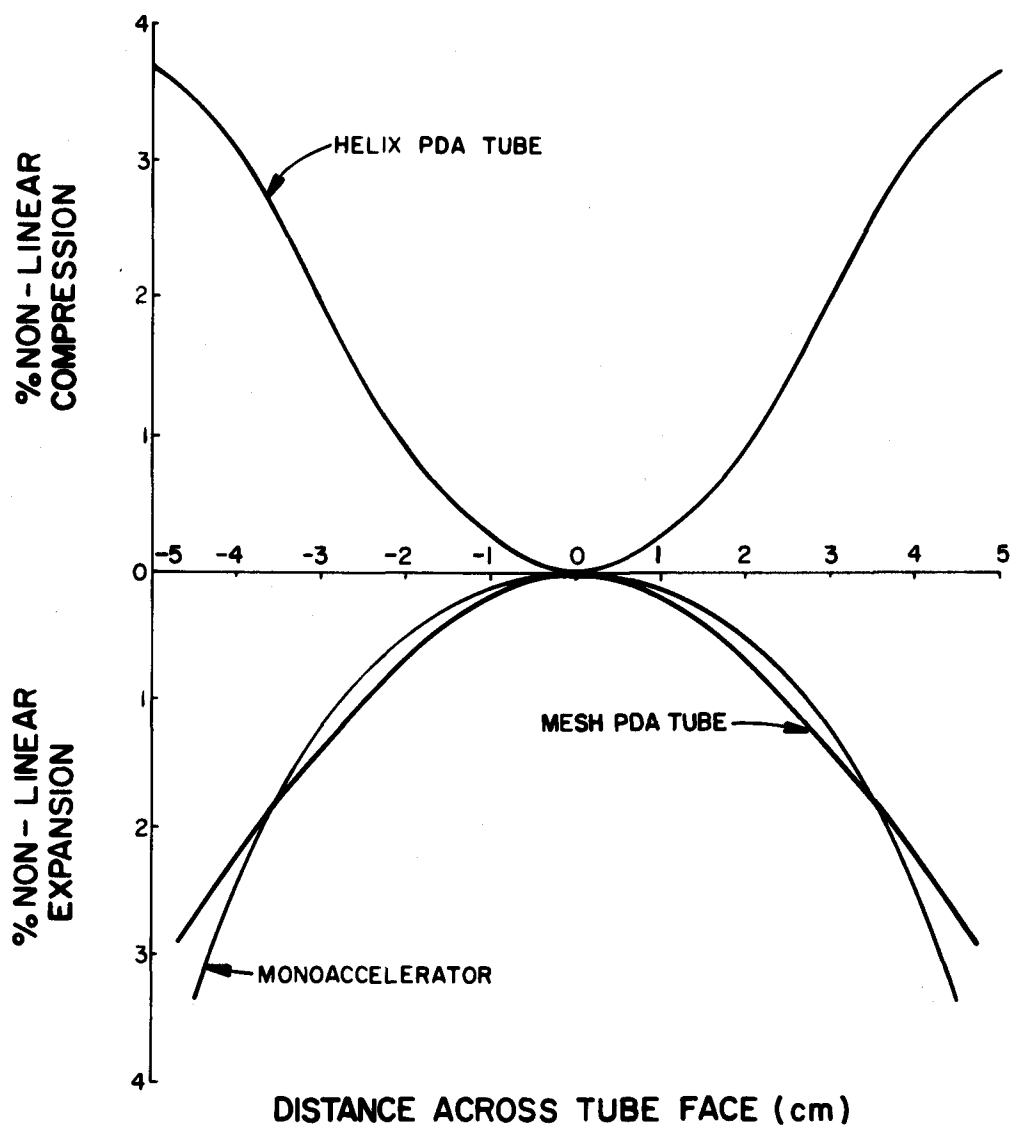


FIG. 24
COMPARISON OF LINEARITY CHARACTERISTICS

itself. The increase in performance is also apparent in the writing speed index as shown by Table I. The writing speed index is a relative measure of the energy density at the screen. This figure of merit is used as an estimate of the improvement in photographic writing speed for design changes over a limited voltage range. The voltage range is restricted because of a change in luminance efficiency of the phosphor with voltage. The information writing speed index, a relative measure of the power density at the screen, compares the readability or information content in a fast writing display. In both cases, the performance of the mesh PDA tube stands out over that of the helix PDA tube.

Figure 24 compares the linearity of the mesh tube with the helix system and a monoaccelerator. Again, because of the lack of scan compression, the tube behaves like a monoaccelerator.

Summary

To summarize the comparison, it should be pointed out that this mesh type of CRT is equivalent to, or superior to, the traditional helix type in every respect except for the minimum trace width. The tube is more compact. It is shorter since a larger deflection angle is allowed because deflection defocusing is not as severe. It also lends itself well to a rectangular design, since the PDA field can be fore-shortened or terminated before the electrons reach the screen. It should be reported that the mesh-type PDA tube has quickly gained acceptance by the oscillographic industry, since its introduction in

1963, and is commonly found in many styles and sizes scattered throughout the industry.

V. BIBLIOGRAPHY

1. Allard, L. S. 1950. An 'ideal' post deflexion accelerator CRT. *Electronic Engineering* 22: 461-463.
2. Bramley, J. 1956. Post-acceleration cathode ray tube. U. S. patent 2,827,592. Mar. 18, 1958.
3. Christaldi, P. S. 1945. Cathode-ray tubes and their applications. *Proceedings of the Institute of Radio Engineers* 33: 373-381.
4. Dolon, Paul J. and Wilfrid K. Niklas. 1960. Electron transmission of mesh lenses for scan magnification in television pictures tubes. *Journal of the British Institute of Radio Engineers* 20: 911-919.
5. DuMont, Allen B. 1932. An investigation of various electrode structures of cathode ray tubes suitable for television reception. *Proceedings of the Institute of Radio Engineers* 20: 1863-1877.
6. Epstein, D. W. 1940. Cathode ray tube. U. S. patent 2,315,367. Mar. 30, 1943.
7. Fischman, M. 1959. Cathode ray tube. U. S. patent 3,035,203. May 15, 1962.
8. Frenkel, L. 1957. Cathode ray tube having post acceleration. U. S. patent 3,023,336. February 27, 1962.
9. deGier, J. 1940. A cathode ray tube with post-acceleration. *Phillips Technical Review*. 5: 245-252.
10. Graupner, H. 1934. Der Einfluss des Beschleunigungsgitters auf die Schreifscharfe des Kathodenoszillographen. *Archiv fur Elektrotechnik* 28: 727-728.
11. Grossbohl, H. W. and K. A. Hoaglund. 1953. Improved instrument cathode-ray tube design. In: *Proceedings of the National Electronics Conference, Chicago*. Vol. 9. National Electronics Conference, Inc., 1954. p. 414-421.
12. Harris, Forest K. 1934. A new cathode-ray oscillograph and its application to the study of power loss in dielectric materials. *Bureau of Standards Journal of Research* 12: 87-102.
13. Hoaglund, K. A. 1951. Cathode ray tube. U. S. patent 2,743,391. April 24, 1956.

14. Howes, D. E. 1924. Cathode ray oscillograph. U. S. patent 1,810,018. June 16, 1931.
15. Iams, Harley. 1939. A fixed-focus electron gun for cathode-ray tubes. Proceedings of the Institute of Radio Engineers 27: 103-105.
16. Klemperer, Otto. 1953. Electron Optics. 2d ed. Cambridge, Cambridge University Press. 471 p.
17. Law, H. B., L. Davne and E. G. Ramberg. 1961. The enhanced-scan, post-acceleration kinescope. RCA Review 22: 603-622.
18. Lempert, Irving E. and Rudolf Feldt. 1946. The 5RP Multiband tube: an intensifier-type cathode ray tube for high-voltage operation. Proceedings of the Institute of Radio Engineers and Waves and Electrons 34: 432-440.
19. Maloff, I. G. and D. W. Epstein. 1934. Theory of electron gun. Proceedings of the Institute of Radio Engineers 22: 1386-1411.
20. Ming, K. J. 1965. A review of methods of post deflexion acceleration used in instrument cathode-ray tubes. Electronic Engineering 37: 94-97.
21. Owren, H. M. 1959. High sensitivity cathode-ray tube. U. S. patent 3,042,832. July 3, 1962.
22. Parr, G. and O. H. Davie. 1959. The cathode-ray tube and its applications. 3d ed. New York, Reinhold. 433 p.
23. Pierce, J. R. 1941. After-acceleration and deflection. Proceedings of the Institute of Radio Engineers 29: 28-31.
24. Rider, John F. and S. D. Uslan. 1959. Encyclopedia on cathode-ray oscilloscopes and their uses. 2d ed. New York, J. F. Rider Publishing. 1 vol.
25. Rogowski, W. and H. Thielen. 1939. Uber Nachbeschleunigung bei Braunschens Rohren. Archiv fur Elektrotechnik 33: 411-417.
26. Schlesinger, Kurt. 1956. Progress in the development of post-acceleration and electrostatic deflection. Proceedings of the Institute of Radio Engineers 44: 659-667.
27. Simpson, Larry R. 1963. CRT design engineering manager, Tektronix, Inc. Unpublished derivation of writing speed index. Beaverton, Oregon. Tektronix, Inc.

28. Soller, Theodore, Merle A. Starr and George E. Valley, Jr. (eds.). 1948. Cathode ray tube displays. New York, McGraw-Hill. 746 p. (Massachusetts Institute of Technology Radiation Laboratory Series, Vol. 22)
29. Spangenberg, Karl R. 1948. Vacuum tubes. New York, McGraw-Hill. 860 p.
30. Sponsler, George C. 1955. Trajectory-tracer study of helix- and band-type post deflection acceleration. Journal of Applied Physics 26: 676-682.
31. Schwartz, E. 1933. High vacuum cathode ray tube. U. S. patent 2,123,636. July 12, 1938.
32. Smith, H. M. 1950. Cathode ray type of discharge device. U. S. patent 2,580,250. Dec. 25, 1951.
33. White, W. G. 1949. Cathode-ray tubes with post-deflection acceleration. Electronic Engineering 21: 75-79.

APPENDIX

VI. APPENDIX

The photographic writing speed of a CRT is a function of many factors. These include the design of the electron gun; e.g., the trace width, beam current, and operating voltage; the phosphor characteristics; e.g., conversion efficiency and spectral match to the film; the recording system; e.g., lens speed and film sensitivity including the spectral response.

This multitude of factors made it desirable to have a relative measure of writing speed that is dependent principally on factors associated with the electron gun or electron optical design and independent of the phosphor and camera recording system.

A relative measure of writing speed can be derived using the three principle tube measurements of accelerating voltage, beam current and spot size or trace width. This derivation is adapted from Simpson (1963).

Consider a small unit area A much less than the cross-sectional area of a beam of total current I_b distributed uniformly across the beam with beam diameter = D .¹ Since the phosphor converts the kinetic energy of the electrons into radiant energy, it is necessary to know

¹Actually, current is not uniformly distributed across the beam diameter, but has roughly a Gaussian distribution. See Figure A-1.3. However, it is expected that substitution of a Gaussian expression for current density distribution would not significantly affect this figure of merit or, at most, give a small increase.

Note that $J_r = J_{\text{peak}} e^{-kr^2}$ in Figure A-1.3.

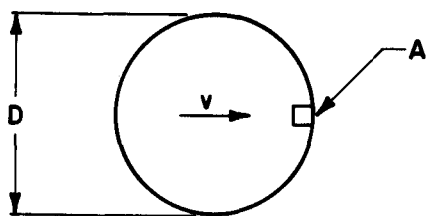


FIG. A1.1

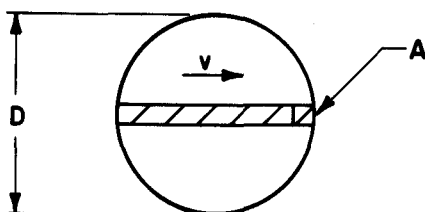


FIG. A1.2

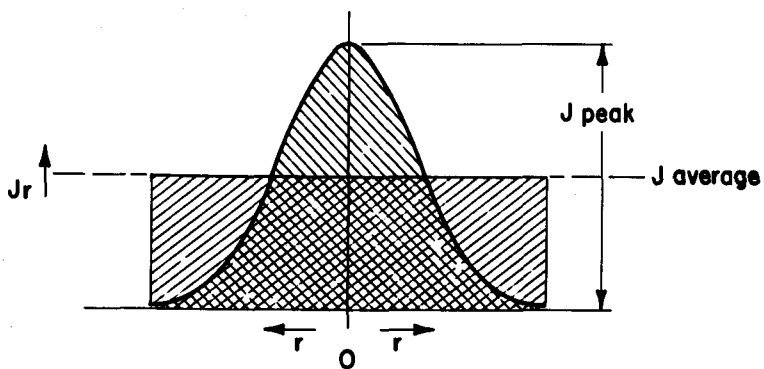


FIG. A1.3

FIG. A1

RELATING BEAM PARAMETERS TO WRITING SPEED CALCULATIONS

the total energy delivered to the small area A by a beam passing over it with a velocity v. This is shown in Figure A-1.1.

The increment of energy, dE, possessed by an increment of charge, dQ, is given by $dE = dQV$ where V is the accelerating voltage. It is remembered that

$$1 \text{ volt} = \frac{1 \text{ joule}}{1 \text{ coulomb}} .$$

The total energy of many charges is:

$$E = \int_0^Q V dQ \quad \text{joules,}$$

$$\text{but, } I = \frac{dQ}{dt}, \quad 1 \text{ ampere} = \frac{1 \text{ coulomb}}{1 \text{ second}},$$

so $dQ = I dt$ and $E = \int_0^T V I dt$, the expression for the total energy

delivered by a current I at a voltage V during time T.

However, only the total energy arriving at the unit area A is of interest so instead of using total current, use the current per unit area = $\frac{I_b}{\frac{\pi D^2}{4}}$ in the integral

$$\text{then } \frac{E}{A} = \frac{4}{\pi} \int_0^T \frac{I_b}{D^2} V dt \quad \frac{\text{joules}}{\text{unit area}} .$$

Since a round beam is being considered, the most energy will be delivered to the unit area transversed by the beam diameter. The time T required for the beam to traverse the unit area is $T = \frac{D}{V}$ as shown in Figure A-1.2.

$$\text{Therefore, } \frac{E}{A} = \frac{4}{\pi} \int_0^{D/V} \frac{I_b}{D^2} v dt$$

$$\text{Evaluating } \frac{E}{A} = \frac{4}{\pi} \left[\frac{I_b}{D^2} vt \right]_0^{D/V} = \frac{4}{\pi} \frac{I_b}{D^2} v \frac{D}{v} = \frac{4}{\pi} \frac{I_b}{D} v \frac{1}{v}$$

which is the energy per unit area delivered by the electron gun.

From the formula $\frac{E}{A} = \frac{4}{\pi} \left(\frac{I_b}{D} v \right) \frac{1}{v}$, it is apparent that the factor $\left(\frac{I_b}{D} v \right)$ contains the parameters of the electron gun.

This factor $\left(\frac{I_b}{D} v \right)$, a measure of the energy density, has been designated Writing Speed Index (WSI). An interpretation is that for the same sweep velocity and the same phosphor screen, the electron optic system having the highest WSI will have the fastest linear writing speed.

For purposes of ease of comparison, it is convenient to have the WSI number between 1 and 10 by using the following form for the equation.

$$WSI = \frac{I_b \text{ (}\mu\text{amp)} \times V_T \text{ (kV)}}{T.W. \text{ (mils)} \times 10}$$

In practice, this index is a reasonable estimate of writing speed changes as the design is modified.

Table A-1 compares the relationship between the photographic writing speed ratios and the WSI ratios for the high performance tubes. The correspondence between the ratios is well within the measurement

TABLE A-1. COMPARATIVE TABLE FOR EVALUATING WRITING SPEED INDEX

	<u>Photo W.S.</u>	<u>WSI</u>
$\frac{\text{improved helix PDA}}{\text{helix PDA}}$	$\frac{770}{700} = 1.1$	$\frac{1.2}{1.0} = 1.2$
$\frac{\text{mesh PDA}}{\text{helix PDA}}$	$\frac{1075}{700} = 1.54$	$\frac{1.6}{1.0} = 1.6$
$\frac{\text{mesh PDA}}{\text{improved helix PDA}}$	$\frac{1075}{770} = 1.40$	$\frac{1.6}{1.2} = 1.33$

error of either the photographic writing speed or, to a lesser degree, the trace width (spot size) measurements. The monoaccelerator tube is conspicuously absent from this comparison. A glance at Table I again shows that the WSI is two times that of the helix PDA tube, while the photographic writing speed is only one-third times the helix tube. Although this has not been followed up in detail, most of the difference is contained in a change in apparent luminous efficiency that occurs as the voltage is increased. Under constant current density conditions for a given phosphor type, a three times change in accelerating voltage produces a six to seven times increase in luminance.

The information writing speed index (IWSI) is an additional rating factor that is used to compare the information capacity of a highspeed CRT. It is simply the writing speed index divided by the trace width.

$$IWSI = \frac{WSI}{D} = V \frac{I_b}{D^2} = VJ.$$

It is proportional to the power density at the screen or, at constant voltage, is a measure of the current density delivered to the screen. It is usually considered proportional to the number of bits/sec resolvable on the CRT. This figure of merit would be related to a measurement of the writing speed in terms of trace widths/sec. This type of measurement is used where a maximum amount of information is required from the CRT.

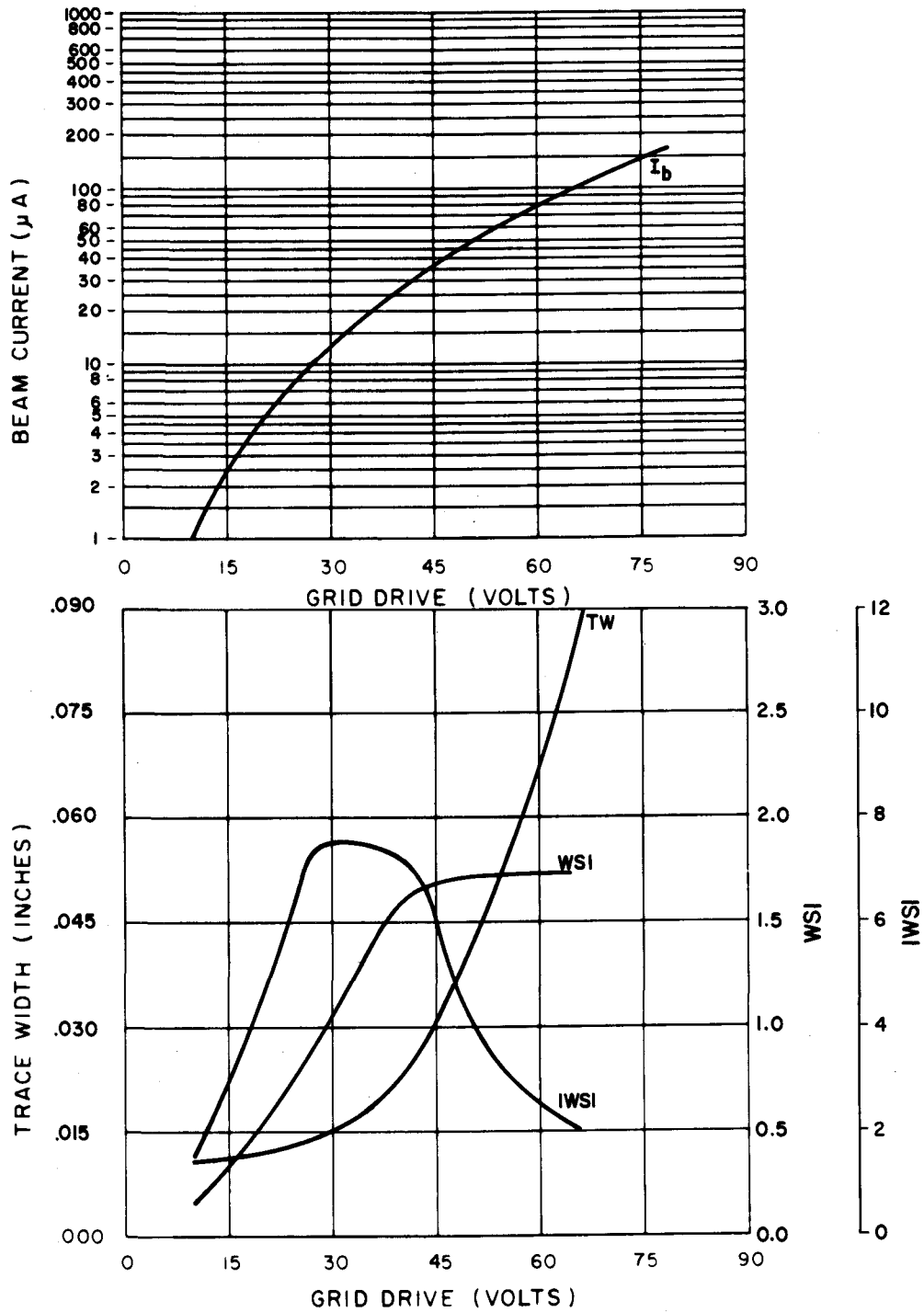


FIG. A2
CALCULATED WRITING SPEED PERFORMANCE

Again, for purposes of ease of comparison, the equation becomes

$$IWSI = \frac{WSI}{T.W. \text{ (mils)}} \times (100)$$

Figure A-1.4 shows clearly that since WSI and IWSI are a function of both beam current and trace width, they depend upon the condition under which the tube is operated. It is also obvious that the maximum information is obtained at some point which is less than the maximum linear writing speed. It is desirable, then, to use both factors as indicators of performance.